Available online at www.sciencedirect.com
SCIENCE DIRECT®
PERGAMON
Polyhedron 22 (2003) 1575–1583
POLYHEDRON
www.elsevier.com/locate/poly

Thermal and structural characterization of a series of homoleptic Cu(II) dialkyldithiocarbamate complexes: bigger is only marginally better for potential MOCVD performance

Silvana C. Ngo, Kulbinder K. Banger, Mark J. DelaRosa, Paul J. Toscano *, John T. Welch *

Department of Chemistry, The University at Albany, State University of New York, 1400 Washington Avenue, Albany, NY 12222, USA

Received 12 November 2002; accepted 24 March 2003

Abstract

A series of Cu(II) dialkyldithiocarbamate complexes, $Cu(S_2CNRR')_2$, with R = R′ = *n*-Bu (**1**); *i*-Bu (**2**); *c*-Hex (**3**); CH_2Ph (**4**); R = *n*-Bu, R′ = Et (**5**); R = *n*-Pr, R′ = *c*-$PrCH_2$ (**6**); R = R′ = *n*-Pr (**7**); *i*-Pr (**8**); allyl (**9**), were prepared. The thermal properties of the complexes were investigated to determine if their potential performance in chemical vapor deposition processes was affected by the nature of the peripheral substituents of the ancillary ligands. Modest gains in volatility were noted for **2** and **7** over the most often utilized complex with R = R′ = Et, while **1** and **8** had thermal parameters and stability comparable to this standard. Unsymmetrical substitution, such as in **5**, also improved volatility, with some loss of stability for this particular compound. X-ray diffraction studies of complexes **1**–**6** suggested that long range Cu···S interactions in the solid-state have little bearing on the thermal properties of this class of Cu(II) complexes.

Keywords: Copper(II) complexes; Dialkyldithiocarbamate ligands; Chemical vapor deposition; Volatility; Crystal structures; Thermal studies

1. Introduction

Metal-organic chemical vapor deposition (MOCVD) is an attractive method for preparing thin films having well-defined composition and morphology for electronic applications [1–7]. For example, Nomura et al. [8,9], among others [10–14], have studied the use of copper(II) dialkyldithiocarbamates, $Cu(S_2CNRR')_2$, as single-source precursors for the growth of semiconducting copper sulfide thin films. In addition, these complexes have been investigated for use as an MOCVD precursor or as a reactant useful for the preparation of single source MOCVD precursors for mixed metal sulfide phases, such as copper–indium sulfide [15–18] or copper-doped cadmium sulfide [19].

For another familiar class of MOCVD precursors, the metal β-diketonates, it is well-known that the steric size of the peripheral substituents of the ancillary ligands can have a profound effect on the performance of the precursor under MOCVD conditions [1,3–5]. While a couple of the previous studies on $Cu(S_2CNRR')_2$ complexes have investigated the effect of increasing the chain length of R and R′ in symmetrically substituted ligands on thermal decomposition properties [9,19], most have concentrated on the complex with R = R′ = Et [8,11,12]. We felt that a more thorough examination of the effect of branched and unsaturated substituents, as well as unsymmetrical substitution of the ancillary ligands, on MOCVD properties was in order, since recent accounts have demonstrated that beneficial changes of physical properties for dialkyldithiocarbamate complexes of copper [14,18] and other metals [10,20–22] can arise from such modifications. Herein, we report on the synthesis and X-ray structural characterization of $Cu(S_2CNRR')_2$, comprising the symmetrically substituted complexes with R = R′ = *n*-Bu (**1**), *i*-

* Corresponding author. Tel.: +1-518-442-3127; fax: +1-518-442-3462.
E-mail addresses: ptoscano@csc.albany.edu (P.J. Toscano), jwelch@uamail.albany.edu (J.T. Welch).

0277-5387/03/$ - see front matter © 2003 Elsevier Science Ltd. All rights reserved.
doi:10.1016/S0277-5387(03)00264-X

Bu (**2**), *c*-Hex (**3**), or CH_2Ph (**4**), and the unsymmetrically substituted complexes with R = *n*-Bu, R′ = Et (**5**) and R = *n*-Pr, R′ = *c*-$PrCH_2$ (**6**). The thermal properties of these six complexes, along with those of the symmetrically substituted complexes R = R′ = *n*-Pr (**7**), *i*-Pr (**8**), or allyl (**9**), were studied by thermogravimetric analysis (TGA) and differential scanning calorimetry (DSC) in order to assess the effect of the peripheral substituents thereon and whether the packing mode of the molecules can be correlated to bulk volatility.

2. Experimental

2.1. Materials and physical measurements

Reagents and solvents obtained commercially were of reagent grade and used as received unless otherwise noted. TGA data were recorded on a TA Instruments TGA 2050 thermogravimetric analyzer under dynamic dry dinitrogen (total flow rate 100 $cm^3\ min^{-1}$), using platinum pans containing a sample size of 1–3 mg, with a ramp rate of 5.0 °C min^{-1}. DSC measurements were obtained using a TA Instruments DSC 2920 differential scanning calorimeter on 1.0–3.0 mg of sample in hermetically sealed aluminum pans (dry N_2 flow rate = 20 $cm^3\ min^{-1}$, 1 atm pressure) at a heating rate of 10.0 °C min^{-1} up to 500 °C and referenced relative to indium. Elemental analyses were performed by MHW Laboratories (Phoenix, AZ).

2.2. General preparation of $Li(S_2CNRR')\cdot 3H_2O$

The procedure follows a modification of the literature method [23]. The appropriate amine (RR′NH; 40 mmol) was added to a stirring slurry of $LiOH\cdot H_2O$ (2.0 g, 48 mmol) in water (3 ml) and CS_2 (3.6 g, 48 mmol) in benzene (10 ml). An exothermic reaction ensued, followed by formation of yellow to orange precipitates. After 1 h, petroleum ether was added and the reaction mixture was filtered. The solids were washed well with petroleum ether and dried in vacuo to give $Li(S_2CNRR')\cdot 3H_2O$ as white to pale yellow solids, which were used in the next procedure without further purification. Typical yields ranged from 70 to 90%.

2.3. General preparation of $Cu(S_2CNRR')_2$ (*1*–*9*)

A solution of $Li(S_2CNRR')\cdot 3H_2O$ (3.2 mmol) in water (40 ml) was added to a stirred solution of $CuCl_2\cdot 2H_2O$ (0.28 g, 1.6 mmol) in water (40 ml). The immediate formation of a brown precipitate was observed. The solid product was filtered, washed with copious amounts of water, and then finally with a small amount of pentane. The crude product was dissolved in diethyl ether (100 ml) and filtered. Evaporation of the solvent gave crystalline black solids, which were dried in vacuo. Yields and elemental analyses for each complex follow:

$Cu[S_2CN(n\text{-}Bu)_2]_2$ (**1**): yield, 64%; *Anal.* Calc. for $C_{18}H_{36}CuN_2S_4$: C, 45.78; H, 7.68. Found: C, 45.85; H, 7.50%.

$Cu[S_2CN(i\text{-}Bu)_2]_2$ (**2**): yield, 91%; *Anal.* Calc. for $C_{18}H_{36}CuN_2S_4$: C, 45.78; H, 7.68. Found: C, 46.00; H, 7.87%.

$Cu[S_2CN(c\text{-}Hex)_2]_2$ (**3**): yield, 75%; *Anal.* Calc. for $C_{26}H_{44}CuN_2S_4$: C, 54.18; H, 7.69. Found: C, 54.21; H, 7.79%.

$Cu[S_2CN(CH_2Ph)_2]_2$ (**4**): yield, 85%; *Anal.* Calc. for $C_{30}H_{28}CuN_2S_4$: C, 59.23; H, 4.64. Found: C, 59.50; H, 4.80%.

$Cu[S_2CN(n\text{-}Bu)(Et)]_2$ (**5**): yield, 69%; *Anal.* Calc. for $C_{14}H_{28}CuN_2S_4$: C, 40.41; H, 6.78. Found: C, 40.47; H, 6.89%.

$Cu[S_2CN(n\text{-}Pr)(c\text{-}PrCH_2)]_2$ (**6**): yield, 70%; *Anal.* Calc. for $C_{16}H_{28}CuN_2S_4$: C, 43.66; H, 6.41. Found: C, 43.78; H, 6.60%.

$Cu[S_2CN(n\text{-}Pr)_2]_2$ (**7**): yield, 74%; *Anal.* Calc. for $C_{14}H_{28}CuN_2S_4$: C, 40.41; H, 6.78. Found: C, 40.64; H, 6.90%.

$Cu[S_2CN(i\text{-}Pr)_2]_2$ (**8**): yield, 58%; *Anal.* Calc. for $C_{14}H_{28}CuN_2S_4$: C, 40.41; H, 6.78. Found: C, 40.49; H, 6.69%.

$Cu[S_2CN(allyl)_2]_2$ (**9**): yield, 86%; *Anal.* Calc. for $C_{14}H_{20}CuN_2S_4$: C, 41.20; H, 4.94. Found: C, 41.05; H, 5.10%.

2.4. X-ray crystallography

Crystals of **1**–**3**, **5** and **6** suitable for X-ray diffraction studies were obtained by slow evaporation of saturated diethyl ether/pentane solutions at ambient temperature, while crystals of **4** were similarly obtained from saturated THF/pentane solution. X-ray data were collected at ambient temperature using a Bruker R3m diffractometer in the $\omega/2\theta$ mode with variable scan speed (3–20 °C min^{-1}, except for **2**: $\theta/2\theta$ mode, 4–20 °C min^{-1}) and graphite monochromated Mo Kα radiation (λ = 0.71073 Å). Check reflections were measured every 200 reflections during data collection and gave no indication of crystal decay. Data were corrected for background, attenuators, Lorentz and polarization effects in the usual fashion [24]. A semi-empirical absorption correction was applied to **1**, **4**, **5**, and **6** using the ψ-scan method.

Structures were solved by direct methods and refined by full-matrix least-squares procedures on $|F^2|$ with SHELXTL-97, version 6.12 [25]. All non-hydrogen atoms were refined anisotropically except for **3**. For **3**, only the heteroatoms and the carbon atom of the chelate ring of

the ligand were refined anisotropically, due to a paucity of data. The peripheral side chains attached to N(1) of the crystallographically full, independent molecule of **6** were disordered; that is, the *n*-Pr and *c*-PrCH$_2$ groups appeared to be superimposed on one another at each site. The disorder was modelled with the *n*-Pr substituent having 55% occupancy on the side involving the C(2) atom and 45% occupancy on the side involving the C(5) atom. The *c*-PrCH$_2$ substituent had the correspondingly opposite occupancies. Hydrogen atom positions were calculated geometrically and fixed at a C–H distance of 0.96 Å and were not refined, with the exception of the hydrogen atoms of the disordered substituents in **6**, the positions of which were neither located nor set. Crystal data and further data collection parameters are summarized in Table 1.

3. Results and discussion

3.1. Synthesis

The homoleptic Cu(II) complexes, Cu(S$_2$CNRR′)$_2$ (R = R′ = *n*-Bu (**1**), *i*-Bu (**2**), *c*-Hex (**3**), CH$_2$Ph (**4**); R = *n*-Bu, R′ = Et (**5**); R = *n*-Pr, R′ = *c*-PrCH$_2$ (**6**); R = R′ = *n*-Pr (**7**), *i*-Pr (**8**), allyl (**9**)) were prepared straightforwardly in high yield via the metathesis of copper(II) chloride with the lithium salt of the dialkyldithiocarbamate ligand. The complexes were purified easily by recrystallization for the X-ray diffraction and thermal studies.

3.2. Thermal studies

TGA data for copper complexes **1**–**9** are collected in Table 2. Experiments were conducted at atmospheric pressure under a nitrogen purge. The temperature of the maximum rate of weight loss (T_{MWL}) was used as a measure of the relative volatilities of the complexes; however, care much be exercised in these cases, since weight loss could be associated with the decomposition, as well as the vaporization of the complexes. For the symmetrically substituted complexes Cu(S$_2$CNR$_2$)$_2$ (R = *n*-Bu, **1**; *i*-Bu, **2**; *n*-Pr, **7**; *i*-Pr, **8**), the TGA traces exhibited single weight loss peaks, with minimal residue, in accord with volatilization being the main thermal event [26]. Surprisingly, the steric size of R has only a small effect on T_{MWL}, though **2** is arguably the best of the four complexes, having the lowest T_{MWL} and leaving essentially no residue. The observed T_{MWL} values for **2** and **7** are ca. 15–20 °C lower than that found for R = Et [27,28]. Unsymmetrically substituted Cu(S$_2$CNRR′)$_2$ (R = *n*-Bu, R′ = Et (**5**) and R = *n*-Pr, R′ = *c*-PrCH$_2$ (**6**)) evaporated somewhat less efficiently, leaving larger residues. Although **5** left a relatively large residue likely indicating that volatilization was accompanied by de-

Table 1
Crystallographic data and parameters for **1**–**6**

	1	**2**
Formula	$C_{18}H_{36}CuN_2S_4$	$C_{18}H_{36}CuN_2S_4$
Formula weight	472.3	472.3
Crystal color, habit	Dark red–brown, plate	Dark brown, parallelepiped
Crystal dimensions (mm)	0.10 × 0.30 × 0.50	0.80 × 0.80 × 0.90
Crystal system	triclinic	monoclinic
Space group	$P\bar{1}$ (No. 2)	$P2_1/n$ (No. 14)
a (Å)	9.212(4)	9.707(3)
b (Å)	9.950(3)	11.241(2)
c (Å)	15.252(6)	12.057(4)
α (°)	71.71(3)	90
β (°)	82.77(3)	101.82(2)
γ (°)	68.03(3)	90
V (Å^3)	1230.9(8)	1287.7(6)
Z	2	2
D_{calc} (g cm^{-3})	1.274	1.218
μ (Mo Kα) (cm^{-1})	12.31	11.77
F(0 0 0)	502	502
2θ max (°)	50.0	55.0
Reflections collected	4495	3052
Independent eflections	4317 (R_{int} = 3.63%)	2926 (R_{int} = 5.26%)
Observed reflections	3026 ($I > 2.0\sigma(I)$)	2211 ($I > 2.0\sigma(I)$)
T_{min}/T_{max}	0.755/0.930	N/A
Number of parameters	226	115
R_1 [a]	0.0480	0.0574
wR_2 [b]	0.103	0.162
Goodness-of-fit on F^2 [c]	1.02	1.06
	3	**4**
Formula	$C_{26}H_{44}CuN_2S_4$	$C_{30}H_{28}CuN_2S_4$
Formula weight	576.4	608.3
Crystal color, habit	Dark brown, parallelepiped	Dark brown, parallelepiped
Crystal dimensions (mm)	0.10 × 0.20 × 0.20	0.25 × 0.30 × 0.30
Crystal system	monoclinic	triclinic
Space group	$C2/c$ (No. 15)	$P\bar{1}$ (No. 2)
a (Å)	18.156(11)	13.855(4)
b (Å)	10.259(7)	14.429(3)
c (Å)	16.206(9)	16.353(3)
α (°)	90	64.94(2)
β (°)	101.40(5)	73.24(2)
γ (°)	90	84.05(2)
V (Å^3)	2959(3)	2835.0(11)
Z	4	4
D_{calc} (g cm^{-3})	1.294	1.425
μ (Mo Kα) (cm^{-1})	10.37	10.88
F(0 0 0)	1228	1260
2θ max (°)	40.0	45.0
Reflections collected	1455	7732
Independent reflections	1370 (R_{int} = 2.96%)	7413 (R_{int} = 6.66%)
Observed reflections	675 ($I > 2.0\sigma(I)$)	4054 ($I > 2.0\sigma(I)$)
T_{min}/T_{max}	N/A	0.886/0.946

Table 1 (*Continued*)

	3	4
Number of parameters	91	667
R_1 [a]	0.0800	0.0745
wR_2 [b]	0.170	0.135
Goodness-of-fit on F^2 [c]	1.03	1.07
	5	**6**
Formula	$C_{14}H_{28}CuN_2S_4$	$C_{16}H_{28}CuN_2S_4$
Formula weight	416.2	440.2
Crystal color, habit	Dark red, hexagonal prism	Brown-red, rectangular prism
Crystal dimensions (mm)	$0.20 \times 0.45 \times 0.50$	$0.20 \times 0.50 \times 0.70$
Crystal system	monoclinic	triclinic
Space group	$P2_1/n$ (No. 14)	$P\bar{1}$ (No. 2)
a (Å)	8.540(1)	8.833(3)
b (Å)	8.637(1)	11.741(4)
c (Å)	13.694(2)	15.555(4)
α (°)	90	90.17(3)
β (°)	93.78(1)	96.91(2)
γ (°)	90	92.29(3)
V (Å^3)	1007.9(2)	1600.1(9)
Z	2	3
D_{calc} (g cm^{-3})	1.371	1.370
μ (Mo Kα) (cm^{-1})	14.93	14.15
$F(0\,0\,0)$	438	693
2θ max (°)	50.0	50.0
Reflections collected	1842	5861
Independent reflections	1765 ($R_{int} = 1.25\%$)	5636 ($R_{int} = 2.50\%$)
Observed reflections	1311 ($I > 2.0\sigma(I)$)	4186 ($I > 2.0\sigma(I)$)
T_{min}/T_{max}	0.536/0.941	0.647/0.994
Number of parameters	97	341
R_1 [a]	0.0450	0.0538
wR_2 [b]	0.113	0.144
Goodness-of-fit on F^2 [c]	1.06	1.04

[a] $R_1 = \Sigma||F_o| - |F_c||/\Sigma|F_o|$.
[b] $wR_2 = [\Sigma w(F_o^2 - F_c^2)^2/\Sigma w(F_o^2)^2]^{1/2}$.
[c] GOF $= [\Sigma w(F_o^2 - F_c^2)^2/(N_{obs} - N_{params})]^{1/2}$, based on F^2 for all data.

composition, this complex demonstrates that the T_{MWL} can be significantly lowered by unsymmetrical substitution of the ligand periphery, a factor which has been recently exploited with R = *n*-Hex, R′ = Me [14].

The TGA behavior for **3**, **4**, and **9** was considerably more complex. In each case the TGA was bimodal, having two temperatures of maximum weight loss. For **3**, the *c*-Hex substituents likely add too much to the molecular weight of the complex so that significant decomposition occurs simultaneously with volatilization. On the other hand, the reactive peripheral substituents in **4** and **9** seem to lead to easier decomposition pathways, with little or no volatilization as suggested by DSC data (vide infra). In these latter two cases, the observed amount of residue is very close to that predicted for CuS based on the composition of the complexes [9,27].

For the DSC studies, the samples were heated under a dinitrogen atmosphere, using hermetically sealed aluminum pans, to eliminate weight loss associated with sublimation. All complexes, except for **3**, showed two endotherms (Table 2). The first, sharp endotherm is attributed to melting. The melting points that we obtained for compounds that have been previously reported were in good agreement with literature values [9,26,27,29].

The second, broader endotherm in the DSC traces of these compounds is more controversial and has been alternatively assigned to volatilization or decomposition [26–29]. We argue that it likely can be assigned to either of these processes or a combination of both, depending upon the complex. For **1**, **2**, **8**, and **9**, the temperature of the second endotherm in the DSC trace for these complexes is close to the T_{MWL} in the TGA experiments, even taking into account uncertainty introduced by the broadness of the DSC absorption. Given this correspondence, and since little residue remains in the TGA studies for these complexes, the second endotherm is likely associated with volatilization. For **3**, **5**, and **6**, there is also fair to excellent agreement between the temperature of the second DSC endotherm and T_{MWL}; however, the larger residues suggest that significant decomposition is occurring along with volatilization. The data for **4** and **9** indicate that decomposition happens with little volatilization. In fact, large exotherms were observed in the DSC trace of **9** at temperatures near T_{MWL}, showing that this complex decomposes readily and is probably too unstable for use in MOCVD applications.

3.3. X-ray diffraction studies

White and coworkers have previously noted that the solid-state structures of homoleptic Cu(II) dialkyldithiocarbamate complexes can roughly be broken down into two classes as a function of the dominant packing forces that are present [30]. In the first, the molecules of complex pack as centrosymmetric dimers with long Cu ···S contacts involving a fifth apical coordination site on one molecule and a sulfur atom from the other molecule of the pair and vice versa. In the second type of packing, the molecules pack as monomers with intermolecular H ···S contacts as the dominant solid-state interaction. These workers concluded that the intermolecular interactions in both cases must be comparable in energy [30]. In the present study, we have found examples of both types of solid-state packing motif, as well as one example that includes both dimeric and monomeric structural types simultaneously and one example that

Table 2
TGA and DSC data for $Cu(S_2CNRR')_2$, (**1**–**9**)

Cu(II)	Substituents	TGA			DSC
Complex	R, R′	T_{MWL}[a](°C)	Weight loss (%)	Residue (%)	Endotherms (°C)
1	*n*-Bu, *n*-Bu	286	98.4	1.6	57; 273
2	*i*-Bu, *i*-Bu	273	99.9	0.1	148; 283
3	*c*-Hex, *c*-Hex	216; 285	16.2; 63.7	20.1	278
4	CH_2Ph, CH_2Ph	286; 323	79.6; 6.1	14.3	204; 237
5	*n*-Bu, Et	245	86.0	14.0	66; 244
6	*n*-Pr, *c*-$PrCH_2$	294	91.4	8.6	103; 267
7	*n*-Pr, *n*-Pr	279	97.2	2.8	102; 272
8	*i*-Pr, *i*-Pr	298	95.0	5.0	177; 303
9	allyl, allyl	231; 254	73.7	26.3	82; 100 [b]

[a] Temperature of maximum weight loss.
[b] Exotherms were also observed at 210 and 263 °C.

does not truly fit into either category. Throughout the following discussion, symmetry-related atoms are designated with an 'a' attached to the label, while similar atoms in crystallographically independent molecules of the asymmetric unit of the unit cell are designated with 'primes'.

$Cu[S_2CN(n\text{-}Bu)_2]_2$ (**1**) is emblematic of the first type of packing pattern, namely the dimeric form (Fig. 1), in which the asymmetric unit of the unit cell contains an entire molecule that is half of the centrosymmetric dimer. The crystal studied here corresponds to the 'α-phase' for this compound, reported previously by White and coworkers [30]. Our results ($2\theta_{max} = 50°$) are more precise than in the prior structure determination ($2\theta_{max} = 40°$) and thus, are included here.

Each copper atom of the centrosymmetric dimer of **1** can be considered to have approximately square pyramidal geometry. With the more precise data, we now can say with better confidence that the Cu(1)–S(1) bond, which involves the sulfur atom that bridges between the two copper atoms of the dimer, is slightly, but significantly longer than the remaining three Cu–S distances in the basal plane. The coordination is completed by a long Cu(1)···S(1a) interaction (2.902(1) Å; symmetry transformation: $-x$, $1.0-y$, $-z$) at the apical position of the pyramid. This distance is significantly longer than for $Cu(S_2CNEt)_2$ (2.844(1) Å) [31,32] and $Cu[S_2CN(n\text{-}Pr)_2]_2$ (2.740(1) Å) [32–34], significantly shorter than for $Cu[S_2CN(2\text{-pyridyl})_2]_2$ (3.230(3) Å) [35], but is similar to that for $Cu[S_2CN(allyl)_2]_2$ (2.888(2) Å) [36]; thus, the apical bridging distance between molecules in the dimers seems to be governed at least in part by the steric size of the peripheral substituents of the ligands. For **1**, there is one long H···S interaction of 3.09(1) Å between H(2b) and S(3a) atoms within the dimer. The copper atoms in **1** are 3.783(1) Å distant, somewhat longer than in other, similar dimers (range: 3.42–3.59 Å) [31–36].

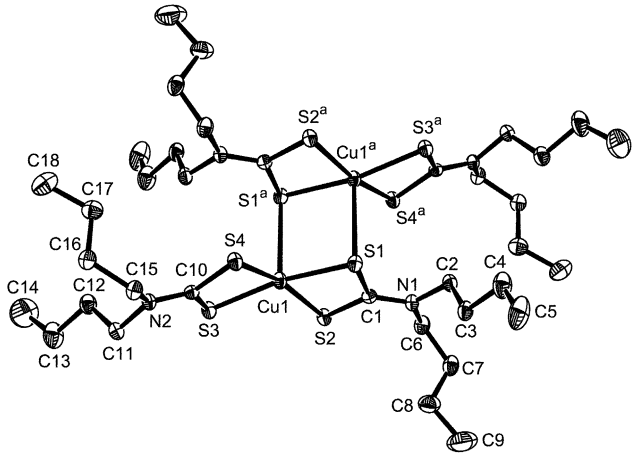

Fig. 1. Molecular structure and atom numbering scheme for dimeric $Cu[S_2CN(n\text{-}Bu)_2]_2$ (**1**). Atoms related by the symmetry transformation ($-x$, $1.0-y$, $-z$) are designated by 'a'. Hydrogen atoms are omitted for clarity.

Even so, the bond lengths (Table 3) in the basal plane of the coordination sphere are not significantly perturbed from those found for the monomeric, square planar complexes (vide infra) and are similar to those found for other dimeric Cu(II) dialkyldithiocarbamates [31–36]. The copper atom is 0.27 Å above the approximate, 'ruffled' basal plane defined by the four sulfur atoms towards the side on which the apical Cu···S interaction occurs. The dihedral angle between the planes defined by the dialkyldithiocarbamate chelates is 156.3(3)°.

Table 3
Selected bond lengths (Å) and angles (°) for $Cu[S_2CN(n\text{-}Bu)_2]_2$ (**1**)

Cu(1)–S(1)	2.323(1)	S(1)–Cu(1)–S(2)	76.7(1)
Cu(1)–S(2)	2.307(1)	S(1)–Cu(1)–S(3)	169.0(1)
Cu(1)–S(3)	2.302(1)	S(1)–Cu(1)–S(4)	102.1(1)
Cu(1)–S(4)	2.301(1)	S(2)–Cu(1)–S(3)	101.2(1)
Cu(1)···S(1a) [a]	2.902(1)	S(2)–Cu(1)–S(4)	164.0(1)
		S(3)–Cu(1)–S(4)	76.9(1)

[a] Symmetry transformation ($-x$, $1.0-y$, $-z$).

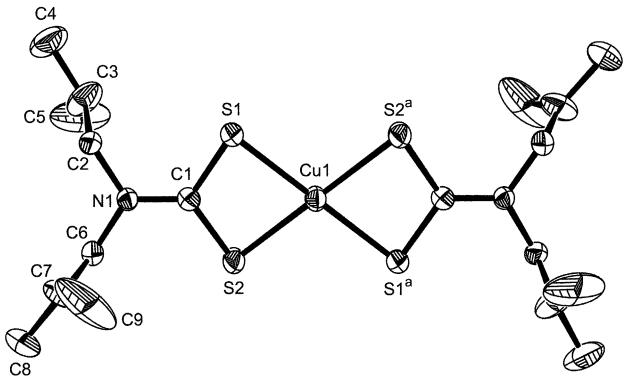

Fig. 2. Molecular structure and atom numbering scheme for $Cu[S_2CN(i\text{-}Bu)_2]_2$ (**2**). Atoms related by the symmetry transformation ($-x$, $-y$, $-z$) are designated by 'a'. Hydrogen atoms are omitted for clarity. The atom numbering schemes for the coordination spheres of $Cu[S_2CN(c\text{-}Hex)_2]_2$ (**3**) and $Cu[S_2CN(n\text{-}Bu)(Et)]_2$ (**5**) are identical (symmetry transformations: ($0.5-x$, $0.5-y$, $-z$) for **3**; ($-x$, $1.0-y$, $1.0-z$) for **5**).

On the other hand, $Cu[S_2CN(i\text{-}Bu)_2]_2$ (**2**) (Fig. 2), $Cu[S_2CN(c\text{-}Hex)_2]_2$ (**3**), and unsymmetrically substituted $Cu[S_2CN(n\text{-}Bu)(Et)]_2$ (**5**) adhere to the second packing motif and are square planar monomers. In each case, the copper atom is situated on a center of symmetry and the asymmetric unit consists of one half of a molecule; as a consequence, the peripheral substituents of **5** adopt the *trans*-geometry. The coordination spheres are perfectly planar as dictated by the crystallographic position of the copper atom. In each case, there are weak, intermolecular H···S interactions in the range 2.91(1)–3.15(1) Å; we find no correlation between the Cu–S bond lengths and these interactions, as speculated for the centrosymmetric β-phase of $Cu[S_2CN(n\text{-}Bu)_2]_2$ [30]. Bond distances and angles (Table 4) in the coordination spheres of **2**, **3**, and **5** are analogous to those in related monomeric complexes, such as $Cu[S_2CN(i\text{-}Pr)_2]_2$ [32,37,38], the 'β-phase' of $Cu[S_2CN(n\text{-}Bu)_2]_2$ [30], $Cu[S_2CN(Me)(Ph)]_2$ [39], $Cu[S_2CN(CH_2)_5]_2$ [40,41], and $Cu[S_2CN(CH_2)_4]_2$ [42] and are slightly, but probably not significantly, shorter on average than for the five-coordinate dimeric Cu(II) complexes (vide supra).

Table 4
Selected bond lengths (Å) and angles (°) for $Cu[S_2CN(i\text{-}Bu)_2]_2$ (**2**), $Cu[S_2CN(c\text{-}Hex)_2]_2$ (**3**), and $Cu[S_2CN(n\text{-}Bu)(Et)]_2$ (**5**)

	2	**3**	**5**
Bond lengths			
Cu(1)–S(1)	2.268(1)	2.281(5)	2.301(1)
Cu(1)–S(2)	2.302(1)	2.304(4)	2.292(1)
Bond angles			
S(1)–Cu(1)–S(2)	77.6(1)	76.8(2)	77.3(1)
S(1)–Cu(1)–S(2a)	102.4(1) [a]	103.2(2) [b]	102.8(1) [c]
S(1)–Cu(1)–S(1a)	180.0 [a,d]	180.0 [b,d]	180.0 [c,d]
S(2)–Cu(1)–S(2a)	180.0 [a,d]	180.0 [b,d]	180.0 [c,d]

[a] Symmetry transformation ($-x$, $-y$, $-z$).
[b] Symmetry transformation ($0.5-x$, $0.5-y$, $-z$).
[c] Symmetry transformation ($-x$, $1.0-y$, $1.0-z$).
[d] Symmetry enforced.

$Cu[S_2CN(n\text{-}Pr)(c\text{-}PrCH_2)]_2$ (**6**) presents the first instance in which *both* five-coordinate, centrosymmetric dimers *and* square planar monomers *co*-crystallize. Here, the asymmetric unit of the unit cell contains an entire, crystallographically independent molecule, which is half of a centrosymmetric dimer, as well as a crystallographically independent half of a four-coordinate monomer. The dimer portion (Fig. 3) has quite typical bonding parameters, including a bridging Cu(1)···S(4a) distance of 2.761(2) Å and a Cu(1)···Cu(1a) separation of 3.596(1) Å. The Cu–S bond lengths in the coordination sphere are virtually uniform (Table 5) with the copper atom 0.29 Å above the, once again, 'ruffled' basal plane defined by the four sulfur atoms. The chelates make a dihedral angle of 152.8(3)°. The *n*-Pr and *c*-$PrCH_2$ substituents of the dialkyldithiocarbamate ligand containing S(1) and S(2) are disordered with nearly equal site occupancies for the two orientations. Thus, there are almost equal populations of the *trans*- and *cis*-geometries, with the former just slightly preferred (see Section 2).

The copper atom of the monomer entity of **6** is situated on a center of symmetry (Fig. 4); the coordination sphere is planar and the peripheral substituents of the ligands adopt the *trans*-geometry according to this crystallographic constraint. Bonding parameters are unremarkable and quite typical for the four-coordinate bonding motif (vide supra). A number of H···S interactions in the range 2.98(1)–3.15(1) Å occur between the dimer and monomer molecules.

Finally, $Cu[S_2CN(CH_2Ph)_2]_2$ (**4**) appears to be exemplar of a packing design not previously observed. The molecules aggregate as weak dimers (Fig. 5), but not in

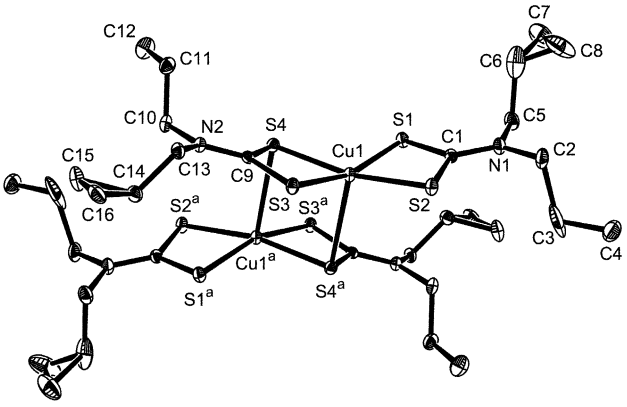

Fig. 3. Molecular structure and atom numbering scheme for the more predominant configuration of the dimeric moiety of $Cu[S_2CN(n\text{-}Pr)(c\text{-}PrCH_2)]_2$ (**6**). Atoms related by the symmetry transformation ($-x$, $1.0-y$, $1.0-z$) are designated by 'a'. Hydrogen atoms are omitted for clarity.

Table 5
Selected bond lengths (Å) and angles (°) for the dimeric (molecule 1) and monomeric (molecule 2) moieties of $Cu[S_2CN(n\text{-}Pr)(c\text{-}PrCH_2)]_2$ (**6**)

Molecule 1			
Cu(1)–S(1)	2.309(1)	S(1)–Cu(1)–S(2)	76.5(1)
Cu(1)–S(2)	2.322(2)	S(1)–Cu(1)–S(3)	162.9(1)
Cu(1)–S(3)	2.323(1)	S(1)–Cu(1)–S(4)	100.0(1)
Cu(1)–S(4)	2.322(1)	S(2)–Cu(1)–S(3)	103.4(1)
Cu(1)···S(4a) [a]	2.761(2)	S(2)–Cu(1)–S(4)	167.8(1)
Molecule 2			
Cu(2)–S(5)	2.276(2)	S(5)–Cu(2)–S(6)	77.0(1)
Cu(2)–S(6)	2.291(2)	S(5)–Cu(2)–S(6a) [b]	103.0(1)
		S(5)–Cu(2)–S(5a) [b]	180.0 [c]
		S(6)–Cu(2)–S(6a) [b]	180.0 [c]

[a] Symmetry transformation $(-x, 1.0-y, 1.0-z)$.
[b] Symmetry transformation $(1.0-x, -y, -z)$.
[c] Symmetry enforced.

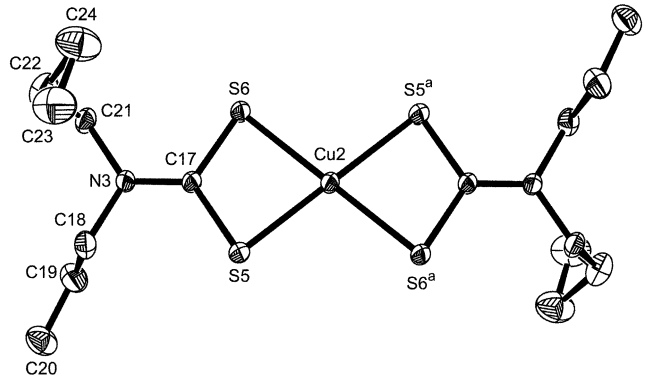

Fig. 4. Molecular structure and atom numbering scheme for the monomeric moiety of $Cu[S_2CN(n\text{-}Pr)(c\text{-}PrCH_2)]_2$ (**6**). Atoms related by the symmetry transformation $(1.0-x, -y, -z)$ are designated by 'a'. Hydrogen atoms are omitted for clarity.

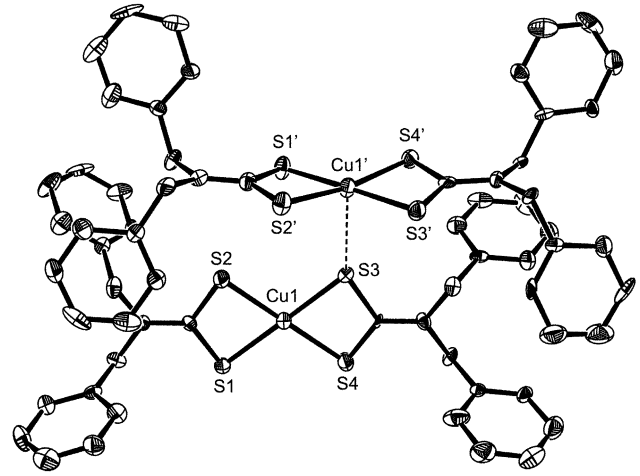

Fig. 5. Molecular structures and atom numbering scheme for the coordination spheres of the two crystallographically independent molecules of $Cu[S_2CN(CH_2Ph)_2]_2$ (**4**). Hydrogen atoms are omitted for clarity.

the manner of the centrosymmetric dimer units described above for **1** and the crystallographically independent dimer molecule of **6**. For **4**, the plane of the coordination sphere of the first, crystallographically independent molecule of the dimer (Fig. 5; primed labels) is approximately perpendicular to the plane of the coordination sphere of the second independent molecule (Fig. 5; unprimed labels), with a dihedral angle between these planes of 88.8(3)°. There is *only one* weak Cu···S interaction between Cu(1′) and S(3) at a distance of 3.468(3) Å. The four sulfur donor atoms for the molecule with the fifth coordination interaction (primed labels) form a relatively unruffled, planar coordination sphere (Table 6), with the copper atom 0.086 Å out of this plane towards S(3); the dihedral angle between the planes defined by the chelate ligands (168.3(3)°) indicates some puckering. The four-coordinate moiety of the dimer (unprimed labels) has close to expected values for a square plane (Table 6), with the copper atom essentially in the plane of the four sulfur donors; the two planes defined by the ligands are nearly coincident (dihedral angle 174.5(3)°). Bond lengths and angles in the coordination spheres of both crystallographically independent molecules are unexceptional. There are several intermolecular H···S interactions in the 3.02(1)–3.18(1) Å range.

At this point, we can make some observations on packing and solid-state aggregation tendencies for Cu(II) dialkyldithiocarbamate complexes. If the copper atom occupies a general position in the unit cell, one generally observes a centrosymmetric, dimeric association, which contains mutual Cu···S interactions between the two metal centers. In this solid-state motif, the coordination planes of the two molecules of the dimer are approximately parallel to each other and necessarily are oriented such that the axes containing the nitrogen atoms of the ligands are also parallel. This packing pattern has been seen for $Cu(S_2CNRR')_2$ in the present

Table 6
Selected bond lengths (Å) and angles (°) for the two crystallographically independent molecules of $Cu[S_2CN(CH_2Ph)_2]_2$ (**4**)

Molecule 1			
Cu(1)–S(1)	2.301(3)	S(1)–Cu(1)–S(2)	77.9(1)
Cu(1)–S(2)	2.279(3)	S(1)–Cu(1)–S(3)	179.5(1)
Cu(1)–S(3)	2.291(3)	S(1)–Cu(1)–S(4)	102.9(1)
Cu(1)–S(4)	2.286(3)	S(2)–Cu(1)–S(3)	101.7(1)
		S(2)–Cu(1)–S(4)	178.8(1)
		S(3)–Cu(1)–S(4)	77.6(1)
Molecule 2			
Cu(1′)–S(1′)	2.264(3)	S(1′)–Cu(1′)–S(2′)	77.7(1)
Cu(1′)–S(2′)	2.304(3)	S(1′)–Cu(1′)–S(3′)	178.1(1)
Cu(1′)–S(3′)	2.286(3)	S(1′)–Cu(1′)–S(4′)	102.1(1)
Cu(1′)–S(4′)	2.317(3)	S(2′)–Cu(1′)–S(3′)	103.0(1)
Cu(1′)···S(3)	3.468(3)	S(2′)–Cu(1′)–S(4′)	170.0(1)
		S(3′)–Cu(1′)–S(4′)	77.5(1)

study with R = R′ = *n*-Bu **1** (the so-called 'α-phase' [30]) and previously for R = R′ = Et [31,32], *n*-Pr [32–34], allyl [36], and 2-pyridyl [35]. The only exception that occurs is for **4** with R = R′ = CH_2Ph; here, as discussed above, we observed a dimer consisting of two crystallographically independent molecules with both copper atoms sited on general positions and with only *one* weak Cu···S interaction. The planes of the coordination spheres are approximately orthogonal to each other in this case.

Alternatively, the copper atom of $Cu(S_2CNRR')_2$ might be situated on a center of symmetry, which generally results in a square planar monomeric complex with no long-range Cu···S interactions. This motif was observed by us for **2** (R = R′ = *i*-Bu), **3** (R = R′ = *c*-Hex), and **5** (R = *n*-Bu, R′ = Et), as well as previously for R = R′ = *i*-Pr [32,37,38], *n*-Bu ('β-phase') [30], R = Me, R′ = Ph [39] and the piperidine [40,41] and pyrrolidine [42] analogues. The only exception here is for R = R′ = Me, where the copper atom is sited on a center of symmetry and an infinite chain structure was determined in which each copper atom has two long-range Cu···S interactions with two symmetry-equivalent molecules on either side of its coordination sphere along the *c* direction [43]. The coordination spheres of the molecules in the chain are approximately parallel; however, the orientation is such that the axes containing the nitrogen atoms of the ligands are approximately orthogonal to each other for each pair of molecules in the infinite chain [43]. This may be a unique case, given the small size of the peripheral Me substituents.

Thus, there are two main packing motifs observed for $Cu(S_2CNRR')_2$. To a degree, larger steric size for the peripheral substituents of the ligands tends to favor packing of the complex molecules as monomers, while smaller groups tend to encourage packing of the metal complexes as dimers. However, other factors are clearly at work as well, such as the solvent of crystallization. For R = R′ = *n*-Bu, a hydrocarbyl group that is intermediate in steric bulk, two different crystalline morphologies have been prepared, namely the 'α-phase', which contains centrosymmetric dimers, and the 'β-phase', which contains well-separated monomers [30]. The former was obtained from the relatively nonpolar solvent mixture of chloroform-light petroleum, while the latter crystals grew from ethanol–chloroform. We also gained the formation of the 'α-phase' from diethyl ether-*n*-pentane mixture. We note that our present study also includes **6** (R = *n*-Pr, R′ = *c*-$PrCH_2$), in which *both* monomer (copper atom on center of symmetry) and centrosymmetric dimer moieties were observed simultaneously in the same crystal. Apparently the unsymmetrically substituted ligand of **6** has peripheral substituents of intermediate size, allowing both solid-state aggregation types to coexist.

4. Conclusions

We have investigated a series of Cu(II) dialkyldithiocarbamate complexes, in the hopes of identifying trends in volatility based on the nature of the peripheral substituents of the ancillary ligands. In particular, we were interested in whether increased steric bulk of these substituents might mitigate Cu···S interactions in the solid-state, thereby increasing the volatility of the complex. We determined the structures of six complexes, including those for which the molecules crystallized as centrosymmetric dimers, as four-coordinate, square planar monomers, as a mixture of these two structural types, and as a newly discovered 'side-on' dimer, in order to assess the importance of such solid-state intermolecular contacts.

The $Cu(S_2CNRR')_2$ complexes with the best characteristics for potential MOCVD application, namely good volatility accompanied by minimal decomposition, were **1**, **2**, **7**, and **8**, which have the substituents R = R′ = *n*-Bu, *i*-Bu, *n*-Pr, and *i*-Pr, respectively. Both **2** and **7** had T_{MWL} values that were lower than that reported for the more studied derivative with R = R′ = Et [27,28], while **1** and **8** were comparable to this compound. Complexes **5** and **6** performed somewhat less efficiently in volatilization experiments, but demonstrated that unsymmetrical substitution of the peripheral ligand positions could lead to even higher volatilities (that is, lower T_{MWL}). Complexes with ligand substituents that were too large (**3**; R = R′ = *c*-Hex), contained phenyl groups (**4**; R = R′ = CH_2Ph), or were too reactive (**9**; R = R′ = allyl), were not suitable for MOCVD applications due to either decreased volatility and/or facile decomposition.

The volatility of the complexes showed little dependence on whether Cu···S interactions were present in the solid-state. Of the four best complexes, **1** and **7** crystallized in the centrosymmetric dimer motif, while **2** and **8** crystallized as four-coordinate monomers, with no long-range Cu···S contacts. White and coworkers have previously suggested that the Cu···S interactions in the dimers are weak and comparable in energy to other intermolecular interactions in the solid-state, based on their ability to crystallize $Cu[S_2CN(n\text{-}Bu)_2]_2$ in each of the two packing modes [30]. Mass spectroscopic studies for $Cu(S_2CNRR')_2$ (R = R′ = Et, *n*-Pr, *n*-Bu, *i*-Bu) [44] and gas-phase electron diffraction studies of $Cu(S_2CNMe)_2$ [45] clearly demonstrate that these complexes are all monomers in the gas phase, no matter the nature of the original solid-state packing pattern. This underscores the general weakness of the Cu···S interactions and the relative ease of overcoming and breaking them; apparently, they have a relative lack of import in determining volatility. Based on our results, it appears that improvements in the volatility of Cu(II) dialkyldithiocarbamate complexes likely will come with the

utilization of unsymmetrically substituted ligands, in which the judicious selection of peripheral substituents according to their steric size and stability, is taken into consideration [14].

5. Supplementary material

Full lists of crystallographic data for **1** (CCDC-196807), **2** (CCDC-196808), **3** (CCDC-196809), **4** (CCDC-196810), **5** (CCDC-196811), and **6** (CCDC-196812), including atomic coordinates, bond lengths and angles, and anisotropic thermal parameters have been deposited with the Cambridge Crystallographic Data Centre. Copies of this information may be obtained from The Director, CCDC, 12 Union Road, Cambridge, CB2 1EZ, UK (fax: +44-1233-336033; e-mail: deposit@ccdc.cam.ac.uk or www: http://www.ccdc.cam.ac.uk).

Acknowledgements

We thank the New York State Science and Technology Foundation and Center for Advanced Thin Film Technology for financial support.

References

[1] T.T. Kodas, M.J. Hampden-Smith (Eds.), The Chemistry of Metal CVD, VCH Publishers, New York, 1994.
[2] J.T. Spenser, Prog. Inorg. Chem. 41 (1994) 145.
[3] S.P. Murarka, S.W. Hymes, Crit. Rev. Solid State Mater. Sci. 20 (1995) 87.
[4] T.J. Marks, Pure Appl. Chem. 67 (1995) 313.
[5] P. Doppelt, Coord. Chem. Rev. 178-180 (1998) 1785.
[6] M.J. Hampden-Smith, T.T. Kodas, A. Ludviksson, in: L.V. Interrante, M.J. Hampden-Smith (Eds.), Chemistry of Advanced Materials, Wiley-VCH, New York, 1998, p. 143.
[7] T.N. Theis, IBM J. Res. Develop. 44 (2000) 379.
[8] R. Nomura, K. Miyakawa, T. Toyosaki, H. Matsuda, Chem. Vapour Depos. 2 (1996) 174.
[9] R. Nomura, K. Kanaya, H. Matsuda, Ind. Eng. Chem. Res. 28 (1989) 877.
[10] S.M. Zemskova, P.A. Stabnikov, S.V. Susoev, I.K. Igumenov, Electrochem. Soc. Proc. 98 (1999) 286.
[11] Y.u. M. Rumyantsev, N.I. Fainer, M.L. Kosinova, B.M. Ayupov, N.P. Sysoeva, J. Phys. IV 9 (1999) 777.
[12] N.I. Fainer, Yu.M. Rumyantsev, M.L. Kosinova, G.S. Yur'ev, E.A. Maksimovskii, S.M. Zemskova, S.V. Sysoev, F.A. Kuznetsov, Inorg. Mater. 34 (1998) 1049.
[13] N.I. Fainer, Yu.M. Rumyantsev, M.L. Kosinova, F.A. Kuznetsov, Electrochem. Soc. Proc. 97 (1997) 1437.
[14] M. Kemmler, M. Lazell, P. O'Brien, D.J. Otway, J.-H. Park, J.R. Walsh, J. Mater. Sci. Mater. Electron. 13 (2002) 531.
[15] R. Nomura, Y. Seki, H. Matsuda, Thin Solid Films 209 (1992) 145.
[16] R. Nomura, Y. Seki, K. Konishi, H. Matsuda, Appl. Organomet. Chem. 6 (1992) 685.
[17] R. Nomura, Y. Seki, H. Matsuda, J. Mater. Chem. 2 (1992) 765.
[18] M. Kemmler, M. Lazell, P. O'Brien, D.J. Otway, Mater. Res. Soc. Symp. Proc. 606 (2000) 147.
[19] S.M. Zemskova, S.V. Sysoev, L.A. Glinskaya, R.F. Klevtsova, S.A. Gromilov, S.V. Larionov, Electrochem. Soc. Proc. 97 (1997) 1429.
[20] P. O'Brien, J.R. Walsh, I.M. Watson, L. Hart, S.R.P. Silva, J. Cryst. Growth 167 (1996) 133.
[21] M.R. Lazell, P. O'Brien, D.J. Otway, J.-H. Park, Chem. Mater. 11 (1999) 3430.
[22] L.A. Glinskaya, S.M. Zemskova, R.F. Klevtsova, J. Struct. Chem. 40 (2000) 979.
[23] A. Uhlin, S. Åkerström, Acta Chem. Scand. 25 (1971) 393.
[24] A. Bruce, J.L. Corbin, P.L. Dahlstrom, J.R. Hyde, M. Minelli, E.I. Stiefel, J.T. Spence, J. Zubieta, Inorg. Chem. 21 (1982) 917.
[25] G.M. Sheldrick, SHELXTL-97, Bruker, Analytical X-ray Instruments Inc., Madison, WI, 2001.
[26] M.L. Riekkola, O. Mäkitie, J. Thermal Anal. 25 (1982) 89.
[27] C.G. Sceney, J.O. Hill, R.J. Magee, Thermochim. Acta 11 (1975) 301.
[28] G. D'Ascenzo, W.W. Wendlandt, J. Thermal Anal. 1 (1969) 423.
[29] S.V. Larionov, L.A. Kosareva, A.F. Malikova, A.A. Shklyaev, Russ. J. Inorg. Chem. 22 (1977) 1299.
[30] P.D.W. Boyd, S. Mitra, C.L. Raston, G.L. Rowbottom, A.H. White, J. Chem. Soc., Dalton Trans. (1981) 13.
[31] M. Bonamico, G. Dessy, A. Mugnoli, A. Vaciago, L. Zambonelli, Acta Crystallogr. 19 (1965) 886.
[32] F. Jian, Z. Wang, Z. Bai, Z. You, H.-K. Fun, K. Chinnakali, I.A. Razak, Polyhedron 18 (1999) 3401.
[33] A. Pignedoli, G. Peyronel, Gazz. Chim. Ital. 92 (1962) 745.
[34] G. Peyronel, A. Pignedoli, L. Antolini, Acta Crystallogr., Sect. B 28 (1972) 3596.
[35] A.M.M. Lanfredi, F. Ugozzoli, A. Camus, J. Chem. Crystallogr. 26 (1996) 141.
[36] E. Kellö, V. Kettman, J. Garaj, Coll. Czech. Chem. Commun. 49 (1984) 2210.
[37] H. Iwasaki, K. Kobayashi, Acta Crystallogr., Sect. B 36 (1980) 1655.
[38] W.E. Hatfield, P. Singh, F. Nepveu, Inorg. Chem. 29 (1990) 4214.
[39] J.M. Martin, P.W.G. Newman, B.W. Robinson, A.H. White, J. Chem. Soc., Dalton Trans. (1972) 2233.
[40] V. Kettman, J. Garaj, Š. Kúdela, Coll. Czech. Chem. Commun. 42 (1977) 402.
[41] (a) J.-P. Lang, J.-M. Lei, G.-Q. Bian, J.-H. Cai, B.-S. Kang, X.-Q. Xin, Jiegou Huaxue 14 (1995) 297;
(b) J.-P. Lang, J.-M. Lei, G.-Q. Bian, J.-H. Cai, B.-S. Kang, X.-Q. Xin, Chem. Abstr., 123 (1995) 131141.
[42] P.W.G. Newman, C.L. Raston, A.H. White, J. Chem. Soc., Dalton Trans. (1973) 1332.
[43] F.W.B. Einstein, J.S. Field, Acta Crystallogr., Sect. B 30 (1974) 2928.
[44] M.L. Riekkola, Acta Chem. Scand. A 37 (1983) 691.
[45] K. Hagen, C.J. Holwill, D.A. Rice, Inorg. Chem. 28 (1989) 3239.